Received: 26 November 2023 | Revised: 21 March 2024 | Accepted: 26 April 2024

DOI: 10.1002/prot.26699

RESEARCH ARTICLE

PROTEINS WILEY

Unraveling the interplay between the leucine zipper and forkhead domains of FOXP2: Implications for DNA binding, stability and dynamics

Cardon Maria Perumal[1] | Monare Thulo[1] | Sindisiwe Buthelezi[2] | Previn Naicker[2] | Stoyan Stoychev[2] | Aasiya Lahki[1] | Sylvia Fanucchi[1]

[1]Protein Structure-Function Research Unit, School of Molecular and Cell Biology, University of the Witwatersrand, Johannesburg, Gauteng, South Africa

[2]CSIR Biosciences, CSIR, Pretoria, Gauteng, South Africa

Correspondence
Sylvia Fanucchi, Protein Structure-Function Research Unit, School of Molecular and Cell Biology, University of the Witwatersrand, 1 Jan Smuts Ave, Braamfontein, 2050 Johannesburg, Gauteng, South Africa.
Email: sylvia.fanucchi@wits.ac.za

Funding information
South African Medical Research Council; National Research Foundation; Royal Society

Abstract

FOXP2 is a transcription factor associated with speech and language. Like other FOX transcription factors, it has a DNA binding region called the forkhead domain (FHD). This domain can exist as a monomer or a domain swapped dimer. In addition to the FHD, the leucine zipper region (LZ) of FOXP2 is also believed to be associated with both DNA binding and oligomerization. To better understand the relationship between DNA binding and oligomerization of FOXP2, we investigated its structure, stability and dynamics, focusing specifically on the FHD and the LZ. We did this by using two constructs: one containing the isolated FHD and one containing both the LZ and the FHD (LZ-END). We demonstrate in this work, that while the FHD maintains a monomeric form that is capable of binding DNA, the LZ-END undergoes a dynamic transition between oligomeric states in the presence of DNA. Our findings suggest that FOXP2's LZ domain influences DNA binding affinity through a change in oligomeric state. We show through hydrogen exchange mass spectroscopy that certain parts of the FHD and interlinking region become less dynamic when in the presence of DNA, confirming DNA binding and oligomerization in these regions. Moreover, the detection of a stable equilibrium intermediate state during LZ-END unfolding supports the idea of cooperation between these two domains. Overall, our study sheds light on the interplay between two FOXP2 domains, providing insight into the protein's ability to respond dynamically to DNA, and enriching our understanding of FOXP2's role in gene regulation.

KEYWORDS
DNA-binding, dynamics, forkhead domain, FOXP2, leucine zipper domain, oligomerization

1 | INTRODUCTION

Forkhead box (FOX) transcription factors are a family of DNA-binding proteins that, like all upstream transcription factors, control the up and down-regulation of specific genes.[1–4] There are over 2000 members that comprise the family of FOX transcription factors which have been identified in over 108 different species.[5] All FOX proteins share a conserved, winged helix DNA-binding domain called the forkhead domain (FHD).[6,7] They are involved in several processes and have varying functions including organogenesis and embryogenesis, metabolic processes, immunity and the maintenance, and function of several tissues.[8–10]

FOXP2 is a member of the FOXP subfamily of FOX transcription factors. This subfamily consists of four members (FOXP1–4), that share two to three structured domains in addition to the FHD. FOXP2 is expressed primarily in the brain and has been associated with speech and language.[11–14] Mutations in FOXP2 proteins lead to widespread dysfunctionality, and result in developmental disorders including autism spectrum disorder. They also have implications in cancer, Parkinson's disease and schizophrenia.[11,14]

Structurally, FOXP2 contains four functional domains: the glutamine rich region which contains a long poly-glutamine tract that has been purported to facilitate protein–protein interactions.[15] The zinc finger domain which could play a role in stabilizing the protein (as its typical function in other transcription factors)[16,17]; the leucine zipper domain (LZ) which has been shown to form homo- and heterodimers in FOXP1, 2, and 4[18,19] and has also been demonstrated to be essential for DNA binding in FOXP3 and other transcription factors[19–21]; and the FHD, the DNA-binding domain of FOXP2, which is responsible for the specificity of DNA binding,[19,22] and has also been shown to form interactions with other proteins.[23] The FOXP FHD, unlike the FHD of other FOX transcription factors, is capable of binding to DNA as a monomer or as a domain-swapped dimer as evident in the crystal structure.[19,24,25] Indeed, of all the FOX transcription factor families, the FOXP subfamily, with their conserved LZ domain as well as a specific and conserved dimer-forming proline to alanine mutation in the FHD[24,25] is the only FOX subfamily that can form dimers. FOXP proteins thus have not one but two dimerization interfaces: the LZ and the FHD which are 134 amino acids apart in the sequence.[17,19,25]

Since FOXP proteins have evolved to oligomerize while the other FOX family members have not, we sought, in this study, to determine what the significance of this unique oligomerization event could be. Since oligomerization of proteins tends to increase their stability, it is plausible that the formation of FOXP2 oligomers will stabilize the protein structure to allow it to perform its function effectively. FOXP proteins may, therefore, regulate transcription of their target genes through oligomerization—directly linking their oligomeric state to DNA binding. Only two domains in FOXP2 have been associated both with oligomerization and with DNA binding and they are the LZ and FHD. In this work we investigate the structure, stability, dynamics, and DNA binding function of these two domains. We make comparisons and draw conclusions on the role of each domain in the mechanism of DNA-binding, thereby elevating and broadening our understanding of the relationship between FOXP2 structure and DNA-binding.

2 | MATERIALS AND METHODS

2.1 | Protein expression and purification

Two protein constructs were used in this study: (i) the isolated FHD of human FOXP2 (residues 504–594). This construct is referred to as FHD throughout this study. We chose this construct because it will provide information specifically on the DNA binding region. (ii) The region of the sequence of human FOXP2 stretching from amino acid 372–715 (the C-terminal end of the protein). This construct incorporates both the leucine zipper and the FHD and is referred to as the LZ-END construct in this study. We chose this construct because it will give information on how the LZ and FHD cooperate together. In addition, the disordered sequence between the two domains and also at the C-terminal region of the protein will be studied in this construct.

T7 *Escherichia coli* cells were transformed with a pET-11a plasmid bearing either the FHD or the LZ-END construct. Cultures were grown to an OD_{600} of 0.6 at 37°C with rotation at 230 rpm and expression was induced with 0.5 mM IPTG. Following induction, FHD was expressed for 22 h at 20°C, while the LZ-END was expressed for 4 h at 30°C. The cultures were then centrifuged at 5000 × *g* for 15 min at 4°C and the pellets were resuspended in equilibration buffer (20 mM Tris–HCl, pH 7.5, 500 mM NaCl, 50 mM imidazole) supplemented with 1 mg mL^{-1} chicken egg yolk lysozyme and 1 mM PMSF and stored at 20°C.

Both constructs were purified via immobilized-metal affinity chromatography using 5 mL HisTrap™ HP IMAC columns, prepacked and charged with Ni Sepharose™ High Performance agarose beads (GE Healthcare Bio-Sciences, Sweden). The proteins were eluted with 20 mM Tris–HCl, pH 7.5, 500 mM NaCl, and 500 mM imidazole. Proteins were sufficiently pure that no further purification was necessary.

2.2 | Oligonucleotides

The FOXP2 FHD binds the following cognate DNA sequence with high affinity: 5′-TGTTTAC-3′.[26] The oligonucleotide was synthesized at IDT® as a double-stranded sequence, bearing unreactive flanking regions on either end: 5′-TTAGGTGTTTACTTTCATAG-3′. The molecular weight of the double-stranded oligonucleotide is 12 230.1 Da.

2.3 | Secondary and tertiary structure assessment

The secondary and tertiary structures of the LZ-END and FHD constructs were assessed in the absence and presence of DNA using circular dichroism and fluorescence spectroscopy respectively. Proteins were dialyzed against a spectroscopy buffer (10 mM HEPES, pH 7.5, and 50 mM Na_2SO_4) and centrifuged at 10 000 × *g* for 5 min, to remove aggregates. The protein concentration was 5 μM and the DNA concentration was 2.5 μM for all experiments with both constructs.

Circular dichroism measurements were taken in triplicate on a J-1500 Circular Dichroism Spectrophotometer at 20°C. Continuous measurements were taken over the wavelength range of 250–180 nm for five accumulations at a speed of 200 nm min^{-1}. Buffer and DNA contributions were subtracted from the triplicate average. Data was reported in terms of mean residue ellipticity (θ_{MRE}). Fluorescence emission spectra were measured on a FP-6300 Jasco fluorescence spectrophotometer at 20°C. Fluorescence measurements were made over the wavelength range of 295–450 nm using an excitation wavelength of 295 nm and bandwidth of 5 nm. Buffer and

DNA contributions were subtracted from the triplicate average of the samples.

2.4 | Quaternary structure assessment

The oligomeric nature of the constructs was assessed using size exclusion chromatography on a HiLoad™ 16/60 Superdex® 75 prep grade column. Each of the constructs was incubated at a concentration of 20 μM in 500 mM NaCl, 10 mM HEPES, pH 7.5, 2 mM DTT for 30 min prior to loading on the column. The molecular weight standards were taken from the Gel Filtration Markers Kit for protein molecular weights 12–200 kDa (Merck, USA).

2.5 | Fluorescence anisotropy

Fluorescence anisotropy was used to derive binding affinities (K_D) of the two constructs for DNA. The experiments were conducted at 20°C on a Perkin Elmer LS-50B Luminescence Spectrometer fitted with an anisotropy filter. DNA oligonucleotide, at 200 nM, was labeled with 5-carboxy-X-rhodamine (ROX) at the 5′ end (Whitehead Scientific (Pty) Ltd., South Africa). The labeled DNA was mixed with increasing concentrations of either the LZ-END or the FHD construct in DNA:protein ratios ranging from 2:1 to 1:40 in sample binding buffer (10 mM HEPES, pH 7.5, and 100 mM NaCl). The excitation wavelength was set at 580 nm and emission at 605 nm. Each experiment was performed in triplicate with 10 technical replicates per measurement. The relative anisotropy (relative to the anisotropy at zero protein concentration) was plotted as a function of increasing protein concentration for each construct and fit to a single-site specific binding model.

2.6 | Hydrogen deuterium exchange mass spectrometry

The hydrogen deuterium exchange mass spectrometry (HDXMS) technique was utilized to monitor the conformational dynamics of LZ-END in the presence and absence of DNA. The labeling, quenching and pepsin cleavage procedures were performed on the PAL HDX system (Leap Technologies, Florida, USA) which is used in conjunction with an Agilent 1100 high-poser liquid chromatography (HPLC) system and Sciex 6600 TripleTOF mass spectrometer. Labeling of the LZ-END protein construct involved incubation of 30 μg LZ-END construct (at time points: 15, 600, and 3600 s), in the presence and absence of 30 μg of DNA (1:1 protein:DNA), in buffer diluted with D_2O to a final concentration of 80% at 20°C. The exchange reaction was then quenched with a two-fold dilution of 3 M guanidinium chloride and 20 mM TCEP, pH 2.5 at 0°C. Controls that were non-deuterated and fully deuterated were also analyzed. For full deuteration, proteins were incubated overnight (18 h) in D_2O at a 80% final concentration. The LZ-END construct was then subjected to pepsin digestion using an online Porozyme immobilized pepsin chromatography column (Applied Biosystems, USA), at 4°C for approximately 30 s and then desalted on an Acclaim PepMap trap column (0.3 × 5 mm) (Thermo Scientific, USA). Subsequently, the protein sample was loaded onto a trap column (LC packing, ID:1.0 mm, phase C18) and then separated using an analytical column of 50 × 2.1 mm C18 (Aeris Peptide 3.6 μm particle size) directly coupled to a TurboIon ESI source of an AB Sciex 6600 TripleTOF MS (AB Sciex, USA). Peptides were eluted using a 10 min 10%–25% acetonitrile gradient, at a flow rate of 200 μL min^{-1}. All columns, pepsin, trap, and analytical were kept at 4°C in a temperature-controlled column oven.

Data Dependant Acquisition (DDA) mode was used for peptide identification on the 6600 TripleTOF. For deuterium labeling only a precursor scan was collected. In DDA mode precursor scans were acquired from *m/z* 360 to 1500 using an accumulation time of 250 ms followed by 30 product scans, acquired from *m/z* 100 to 1800 at 100 ms each, for a total scan time of 3.3 s. Charge ions (1–5, that fall in the mass range 360–1500 *m/z*) were automatically fragmented in Q2 collision cells using nitrogen as the collision gas. Collision energies were chosen automatically as function of *m/z* and charge. Dynamic exclusion was set to 15 s. HDX-MS experiments including the controls were performed in triplicates.

PEAKS Studio version 6 was used to identify peptide peaks and their associated properties, including their sequences, retention times, charge information, and peptide quality scores. The peptide pool produced was imported into the analysis program HD Examiner (Sierra Analytics, USA), which was then used to calculate deuterium uptake for each peptide per time point measured. The parameter summary can be found in Table 1.

2.7 | Equilibrium unfolding

In order to study the stability of the LZ-END and FHD constructs, each construct was denatured in increasing concentrations of urea (ranging from 0 to 9 M) at a final protein concentration of 5 μM. The solutions were left for 1 h so as to reach equilibrium. Urea was prepared in sodium sulfate buffer (10 mM HEPES at pH 7.5 with 50 mM sodium sulfate). The unfolding of both protein constructs was probed using both circular dichroism and fluorescence spectroscopy. The full-spectra measurements were recorded at 20°C using the Jasco FP-6300 fluorescence spectrophotometer and the Jasco J-1500 circular dichroism polarimeter. Data were collected in triplicate and were fit to either a two-state or three-state unfolding model[27] and from this, the thermodynamic parameters $\Delta G(H_2O)$ and *m*-value were calculated.

3 | RESULTS

3.1 | The FHD and LZ-END constructs

The two FOXP2 constructs that were used in this study were chosen because they contain the only two domains in the protein that are

TABLE 1 HDXMS experimental conditions and peptide information.

Dataset	Apo	DNA-bound
Labeling conditions	20 mM Tris, 500 mM NaCl, 50 mM imidazole, pH 7.6, and 20°C	20 mM Tris, 500 mM NaCl, 50 mM imidazole, pH 7.6, and 20°C
Percent D_2O	80%	80%
Time course (s)	15; 600; 3600	15; 600; 3600
Controls	Fully deuterated sample (Apo)	Fully deuterated sample (DNA-bound)
Back exchange % (mean; IQR)	50.68; 23.1	41.96; 18.3
Number of peptides	145	152
Sequence coverage (% amides covered by peptides)	80.1%	80.1%
Average peptide length	17.0	16.2
Peptide redundancy (total peptide/ total amides)	0.58	0.61
Replicates (biological or technical)	3 biological	3 biological
Repeatability (e.g., average stdv of deuterium percent)	5.12	3.98
Significant differences in HDX (change in deuterium uptake)	≥30%	≥30%

associated with both DNA binding and oligomerization. The LZ-END construct is the larger of the two constructs and consists of the 343 amino acids at the C-terminal end of the protein. It contains both the LZ domain and the FHD. The FHD construct consists only of the winged helix DNA binding domain (Figure 1). The LZ-END and FHD constructs were successfully purified (Figure 1) and the molecular weights of the LZ-END and FHD constructs as calculated from SDS-PAGE were ~46 and ~13 kDa respectively which corresponds with their predicted sizes.

3.2 | Structural characterization

The crystal structure of the FHD in the presence of DNA[24] shows both the monomer and the domain swapped dimer bound to the DNA via the recognition helix, H3 (Figure 2). The FHD folds into the winged helix structure which is typical of all FOX FHDs. This structure is also retained in the domain swapped dimer. Since only the FHD of FOXP2 has been crystallized, the structures of the full-length protein as well as of the LZ-END construct were generated in their apo form using AlphaFold[28] (Figure 2). These models show clearly the four structured domains of FOXP2 including the LZ and FHD (which aligns well with the FHD from the crystal structure). However, a large portion of the sequence is predicted to be disordered in these models and the exact structure of these regions is only given with low confidence due to their apparent dynamic nature.

Circular dichroism and fluorescence spectroscopy were used in order to confirm the structural integrity of the two constructs and also to assess whether the inclusion of DNA has any effect on the secondary or tertiary structure respectively (Figure 3).

The circular dichroism spectra of both constructs are characteristic of a predominantly alpha-helical protein with clear troughs at 222 and 208 nm. This result is in keeping with the predicted structures of these proteins (Figure 2). When the constructs are incubated in the presence of DNA, the spectra, while still characteristic of a helical protein, are not fully superimposable with the spectra of the apo constructs. This suggests that DNA causes subtle changes to the backbone of both constructs with the difference being more pronounced in the LZ-END construct compared to the FHD. This is to be expected due to the increase in disordered regions in this construct.

Fluorescence spectroscopy was conducted by selectively exciting the tryptophan residues at 295 nm. The FHD contains three tryptophan residues: Trp533, Trp548, and Trp573. There are no additional tryptophan residues found in the remaining sequence in the LZ-END construct and therefore the fluorescence spectra provide information pertaining to the tertiary structure of only the FHD in both constructs. Indeed, the spectra for the two constructs are very similar which is to be expected. The spectra show two peaks, one at 334 nm and one at 340 nm. This is because the environment of the three tryptophan residues in the FHD is different, with Trp533 and Trp573 being more solvent exposed than Trp548 which is deeply buried in a hydrophobic pocket. The spectra of the constructs in the presence of DNA show significant quenching which has been well documented for the FOXP2 FHD elsewhere.[29] Despite the quenching, the wavelengths of the peaks remain the same, suggesting that the tryptophan microenvironment does not change significantly in the presence of DNA in either construct and the 3D fold of the FHD remains the same in the presence and absence of DNA.

The oligomeric nature of the constructs was investigated using size exclusion chromatography (Figure 4). At a concentration of 20 μM, the FHD is not seen to form the domain swapped dimer and exists as a single monomeric species. Because the LZ-END species is not entirely globular, it is difficult to obtain an accurate size using SEC. However, given that the predicted sizes are more than double the monomeric size of 40 kDa, it is clear that LZ-END is not monomeric. This is expected as the LZ is known to dimerize. The protein exists as a mixture of two species with sizes predicted to be ~120 and ~80 kDa. Since we cannot determine the exact nature of the oligomeric species from SEC, it is sufficient for the purpose of this study

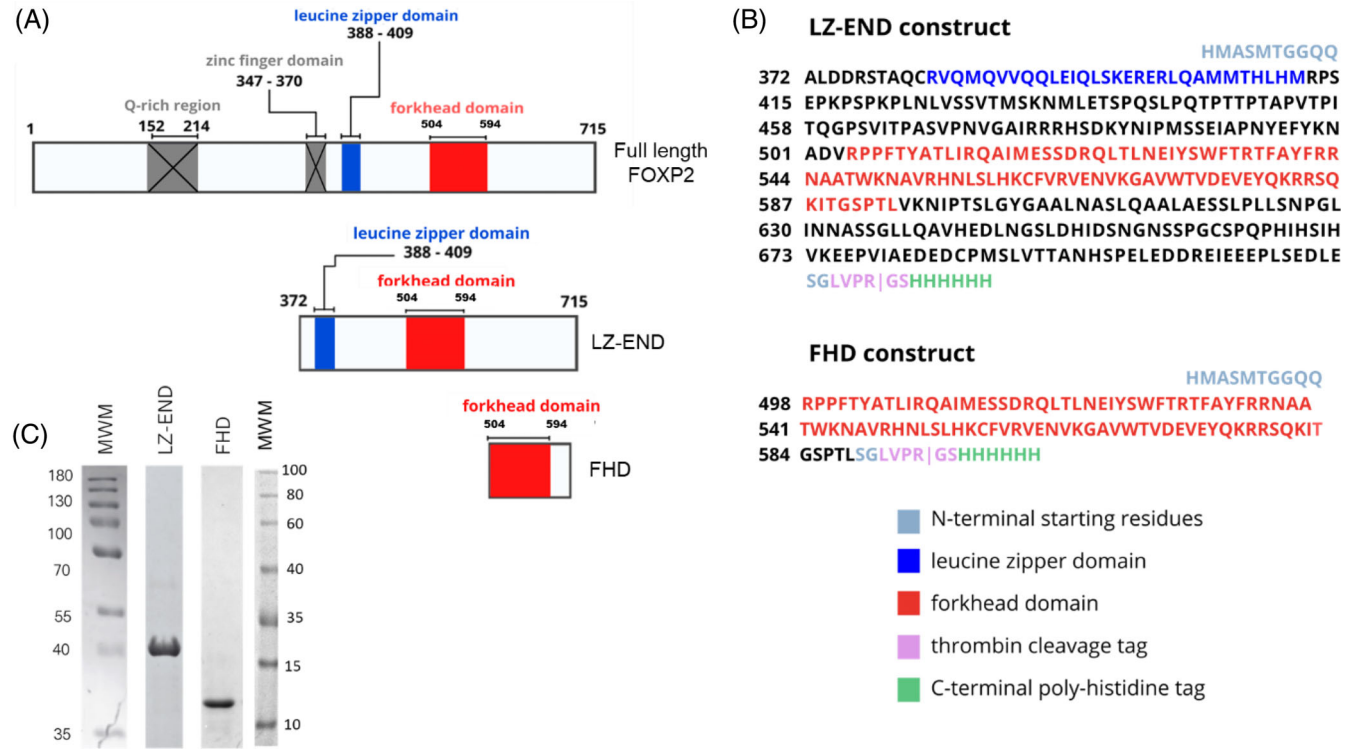

FIGURE 1 FOXP2 domains, experimental constructs, and purity assessment. (A) Full length FOXP2 contains a poly-glutamine region, a zinc finger domain, a leucine zipper domain, and a forkhead domain. The experimental constructs used in this study focus on the leucine zipper and the forkhead domain. The LZ-END construct (40 kDa) is comprised of the stretch of FOXP2 sequence from the leucine zipper domain to the C-terminal end and includes the DNA binding forkhead domain. The FHD construct (13 kDa) consists only of the isolated forkhead domain. (B) The FOXP2 LZ-END sequence spans positions 372–715 and includes: starting residues that make for improved protein expression (gray), the leucine zipper domain (blue), the forkhead domain (red), a thrombin cleavage site (purple), and a poly-histidine tag at the C-terminus (green). The FHD construct spans residues 504–594 (red). (C) Both constructs were successfully purified via immobilized metal-affinity chromatography.

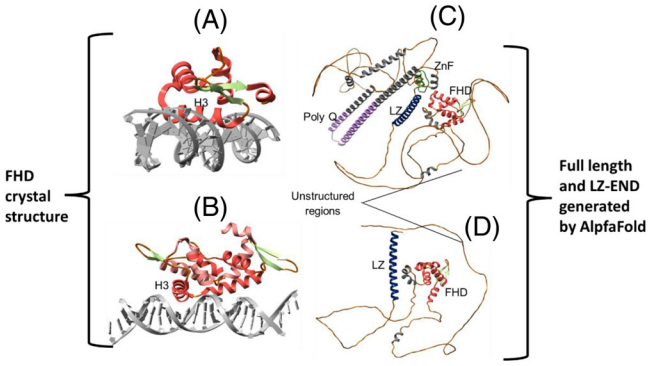

FIGURE 2 Structure of the isolated forkhead domain, the LZ-END construct, and full length FOXP2. The crystal structure of the FHD has been solved in the presence of DNA.[24] Both monomeric (A) and domain swapped dimeric (B) forms of the protein exist and are capable of binding to DNA (PDB: 2A07). The structure of the full-length protein as generated by AlphaFold[28] is shown in (C), with forkhead domain shown in red, leucine zipper domain in dark blue, zinc finger (ZnF) domain in green, and the glutamine rich region in purple. The AlphaFold generated model of the LZ-END construct used in this study, comprising the leucine zipper domain to the end of the FOXP2 sequence is shown in (D). A large proportion of the full-length and LZ-END protein is unstructured and of low confidence in the AlphaFold model.

to recognize that they are two distinct oligomeric species and simply to refer to these as the larger and the smaller oligomeric species which may be suggestive of a trimer and a dimer respectively.

3.3 | DNA-binding

Electrophoretic mobility shift assays (EMSAs) indicate the presence of a protein–DNA complex due to its greater hydrodynamic volume and slower migration in an electric field compared to the free DNA. EMSAs were performed with the FHD and LZ-END constructs incubated with the cognate DNA oligonucleotide. They were done to confirm functionality and hence the correct fold of the protein and also to obtain a qualitative perspective on how the constructs bind DNA.

As seen in Figure 5, both constructs show DNA binding. The FHD binds at a protein:DNA ratio of 5:1 or higher. Only a single shifted band is observed which corresponds with the SEC results and indicates that the monomeric FHD is capable of binding DNA. The LZ-END construct appears to bind with greater affinity than the FHD since electrophoretic shifts are seen at lower protein:DNA ratios than the FHD. Considering the LZ-END construct also contains the FHD in addition to the leucine zipper, this result implies that the leucine

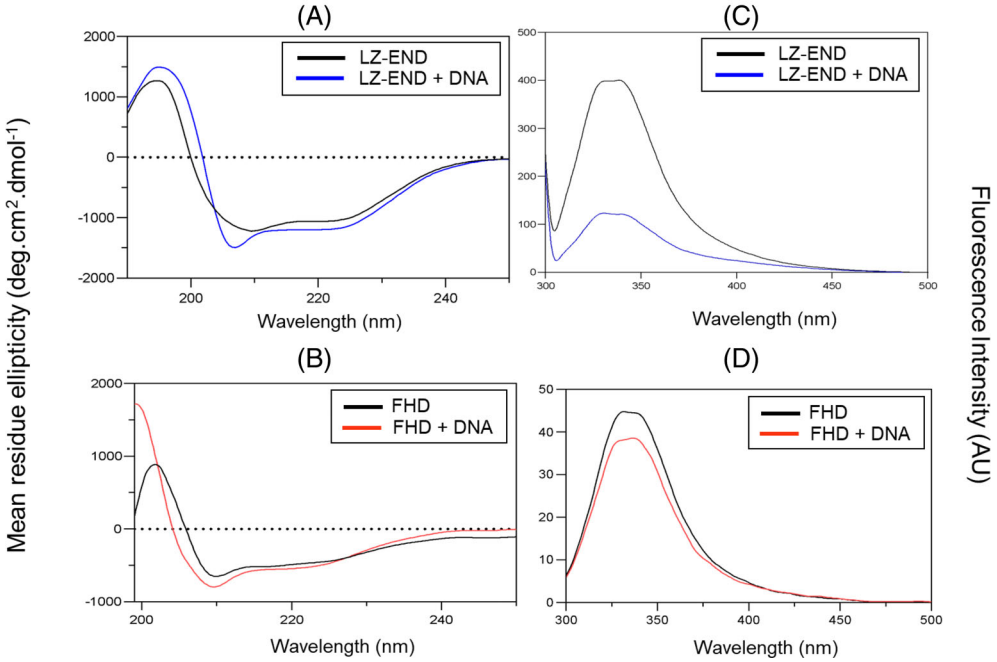

FIGURE 3 Circular dichroism and fluorescence spectroscopy profiles of the LZ-END and FHD constructs in the absence and presence of DNA. The mean residue ellipticity of the apo and DNA-bound constructs was measured over the wavelength range of 180–250 nm for both the LZ-END (A) and the FHD (B) constructs. Protein and DNA concentration was kept at 5 and 2.5 μM respectively for both constructs. The spectra indicate a secondary structure that is predominantly α-helical for both constructs in both the presence and absence of DNA. Fluorescence emission (ex295 nm) of both the apo and DNA-bound complex was monitored over the wavelength range of 300–500 nm for the LZ-END construct (C) and the FHD construct (D). In both cases, DNA causes quenching of the fluorescence intensity, but the wavelength of the peak is not changed.

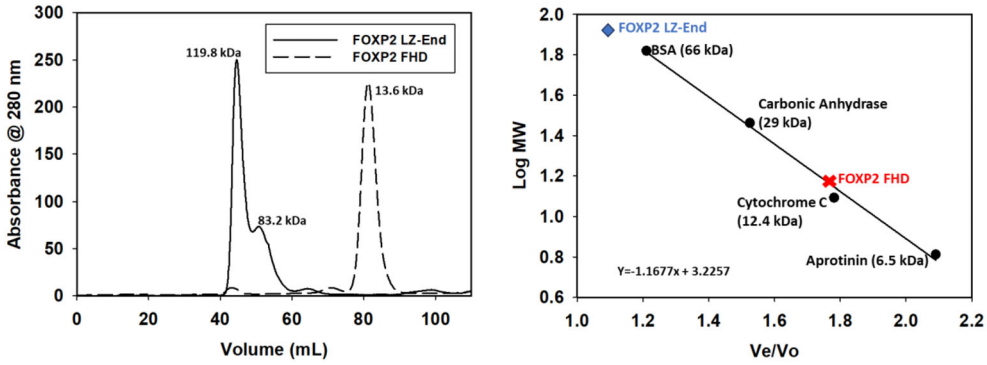

FIGURE 4 Size exclusion elution profile of LZ-END and FHD. 20 μM LZ-END (solid) and FHD (dashed) was separated on a HiLoad™ 16/60 Superdex® 75 column. FHD elutes as a single monomeric species of 13.6 kDa but LZ-END elutes as a higher order oligomer in two peaks suggestive of a trimer and a dimer.

zipper contributes to DNA binding affinity. Interestingly, three distinct shifted bands are resolved (the free DNA band is at the very bottom of the gel). The three shifted bands are indicative of three different protein–DNA species. Since the apo protein exists as a mixture of a larger and a smaller oligomeric species as detected with SEC (Figure 4), the three species seen on the EMSA could represent the larger and smaller oligomer identified with SEC and an additional species that only forms in the presence of DNA. These oligomeric species appear to form as a result of the leucine zipper and not the FHD which remains monomeric even in the presence of DNA.

Following the qualitative assessment of DNA-binding in both constructs through the EMSA studies, the strength of the DNA-binding interaction was studied further using fluorescence anisotropy (Figure 6). Fluorescence anisotropy provides a means of measuring the protein–DNA binding interactions by exploiting the excitation properties of fluorescently labeled DNA that bound to the protein in solution. Principally, the tumbling motion of the heavier labeled DNA–protein complex is slower than the unbound entities which results in increased fluorescence anisotropy which can be measured. The DNA-binding isotherms are fit to a single-site binding model and the affinity of the interaction is calculated in the form of dissociation constants (K_D).

The K_D of the interaction between the FHD and DNA was found to be 1.9 μM while the LZ-END–DNA interaction has a K_D of 0.3 μM.

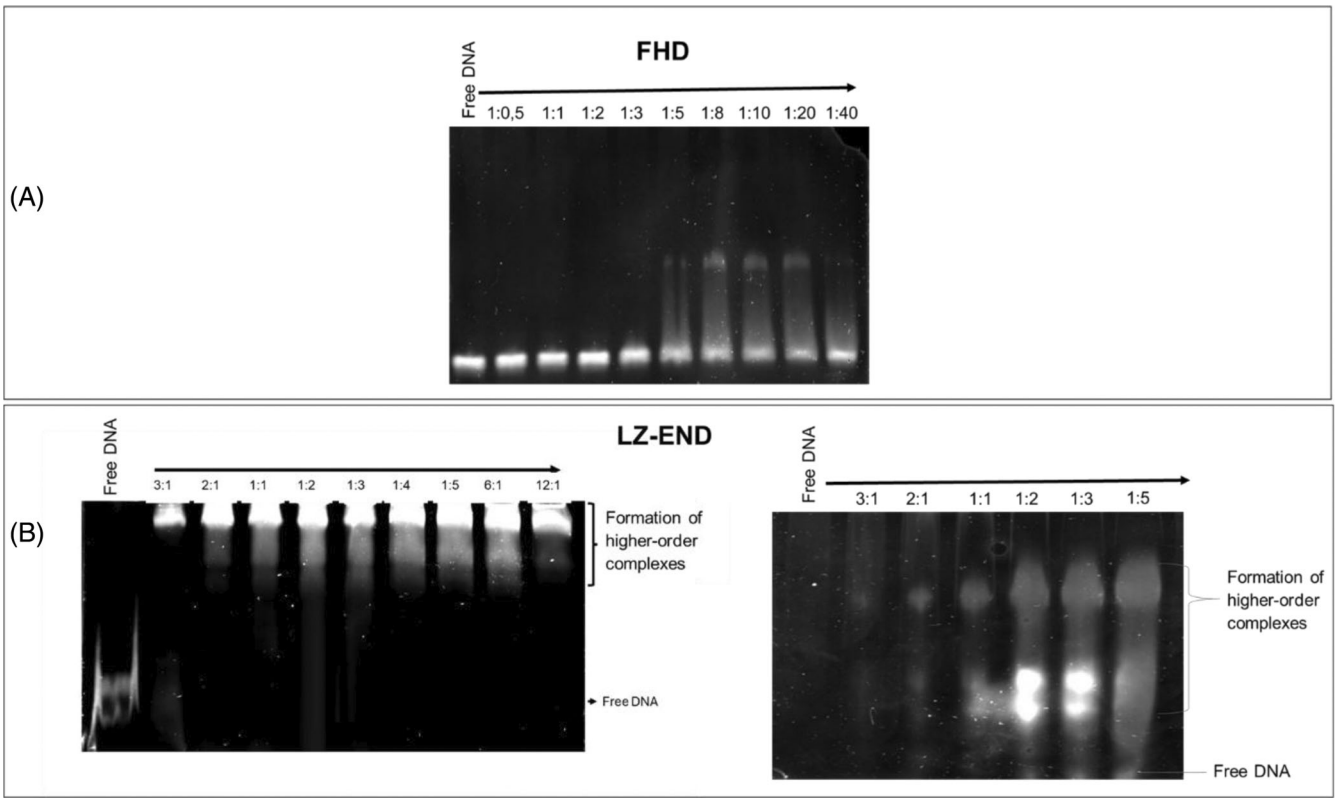

FIGURE 5 Electrophoretic mobility shift assays for the LZ-END and FHD constructs. Increasing concentrations of either the FHD or the LZ-END were incubated with a constant concentration of 1 μM DNA oligonucleotide. The samples were resolved on a non-denaturing 10% (w/v) polyacrylamide gel. For the FHD construct (A), binding is observed from a ratio of DNA: protein of 1:5. For the LZ-END construct (B), binding is observed from a DNA:protein ratio of 3:1. Two gels are shown. The one on the left clearly shows the position of the free DNA on the gel while the one on the right was left to separate for longer so as to show better separation of the higher order species. More than one species of LZ-END binds to the DNA.

This difference indicates that the FHD binds DNA with a 6-fold weaker affinity than the LZ-END construct, a difference that is statistically significant (Figure 6). This result corresponds with the EMSA results. Because both constructs contain the DNA-binding FHD, but the LZ-END construct contains additional disordered regions plus the leucine zipper, the fluorescence anisotropy results suggest that the leucine zipper (and potentially the disordered regions of the sequence) may promote strong DNA-binding in conjunction with the FHD which directs the specificity of the interaction.[30]

3.4 | Conformational dynamics

In order to probe deeper the relationship between FOXP2 and DNA, hydrogen/deuterium exchange mass spectroscopy was performed on the LZ-END construct both in the presence and absence of DNA. From this work we were able to investigate any changes in conformational dynamics upon DNA binding. Since our work shows that the leucine zipper is primarily involved in DNA-binding affinity, assessing its interaction with DNA in this construct, alongside the DNA-binding FHD, provides both a global and local depiction of how these structural motifs dynamically cooperate to ensure DNA binding. Additionally, the dynamics of the randomly coiled unstructured regions also provide evidence of whether or not they participate in the interaction at all.

The rate of deuterium uptake of the apo and DNA-bound LZ-END construct was measured over 15, 600, and 3600 s and compared to the non-deuterated control. Heat maps were constructed for both apo and DNA-bound protein (Appendix S1) and the difference map highlighting regions of difference in dynamics between apo and complexed LZ-END is mapped onto the model structure and shown in Figure 7.

The regions of LZ-END that show the greatest difference in exchange between the apo and DNA-complexed construct are shown in Figure 7. The regions that show significant changes in deuteration over time are the FHD, the leucine zipper, a stretch of interlinking sequence between the LZ and FHD and a portion preceding the acid-rich tail at the C-terminus of the protein. The remaining random coiled sequence in the LZ-END construct shows very little difference in exchange between the apo and the complexed protein and thus is unlikely to be involved in DNA binding. The deuterium uptake plots in Figure 7 show clearly that the regions of LZ-END that exhibit the greatest difference in exchange between DNA-bound and apo forms are H3 and H1 from the FHD as well as the interlinking sequence located between the LZ and FHD. In all three of these regions, the DNA-bound form shows lower deuterium uptake for all time points

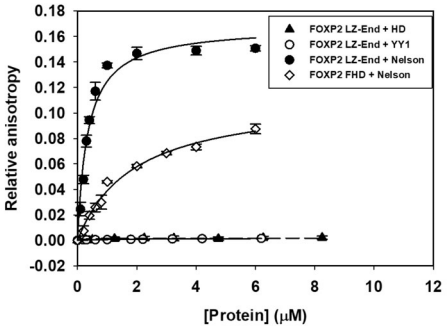

Sample	K_d
FOXP2 LZ-END + non-specific DNA	20.83 ± 0.1953
FOXP2 FHD + non-specific DNA	22.066 ± 0.5917
FOXP LZ-END + Cognate DNA	0.3471 ± 0.0554
FOXP2 FHD + Cognate DNA	1.9040 ± 0.2507

FIGURE 6 Fluorescence anisotropy illustrating the independent binding interaction of the LZ-END and FHD constructs with DNA. For each experiment, 500 nM ROX-labeled dsDNA containing a single FOXP2 binding site was incubated with increasing concentrations of each protein construct (0–6 μM). The data was fitted to a single site binding model. Errors indicate the standard deviation of three averaged replicates. FOXP2 LZ-END (filled hexagons) and FOXP2 FHD (open diamonds) bind specifically to FOXP2 cognate DNA. The K_D calculated for the FHD and the LZ-END were 1.9 ± 0.3 and 0.3 ± 0.06 μM respectively indicating that the LZ-END binds with higher affinity than the FHD. A two-sample *t*-test indicates that there is a statistically significant difference between the K_D values (*p < .05, **p < .01, and ***p < .001). When incubated with non-specific DNA, both FOXP2 LZ-END (filled triangles) and FOXP2 FHD (open hexagons) show no binding.

measured. This means that the backbone of these three regions is more protected from deuterium exchange and the regions are less dynamic in the presence of DNA than in the absence of DNA. Alternatively, the leucine zipper region takes up the same amount of deuterium in both the apo and DNA-bound forms. This region is still of interest, however, because it shows a marked increase in exchange over time implying that it remains dynamic whether in the presence or absence of DNA.

The hydrogen/deuterium exchange results for LZ-END were compared with the results obtained previously for the isolated FHD.[25] Interestingly the dynamics of the FHD region is not identical when in the isolated construct compared to in the longer LZ-END construct. While H3 and H1 show a reduction in deuterium uptake upon DNA binding in both constructs, the remainder of the DNA-bound FHD is more dynamic in the LZ-END construct on average, than in the isolated FHD construct (Figure 8).

3.5 | Stability at equilibrium

Understanding the conformational stability of the constructs will provide deeper insight into the dynamic interplay between the FHD and the leucine zipper domain in the full-length protein which will help us make conclusions about the mechanisms of oligomerization and its relationship to DNA binding. Equilibrium unfolding curves of both constructs are shown in Figure 9. Both fluorescence and circular dichroism were used to probe the unfolding of the constructs by focusing on their tertiary and secondary structures respectively.

Both the FHD and the LZ-END constructs unfold via a two-state transition when unfolding is monitored using fluorescence. Considering the tryptophan residues are located in the FHD in both the FHD and the LZ-END construct, the tryptophan environments will be very similar in both constructs, and it is not too surprising that the fluorescence-monitored transitions are comparable for both constructs. The two-state model assumes that only two conformational states exist along the unfolding transition of both constructs: the native (N) and the denatured (D) states. While the two curves are close to being superimposable, the denaturation mid-point (*Cm*) and the ΔGH_2O are both higher for LZ-END (6.2 M urea and 19.9 kJ mol^{-1} respectively compared to the values of 5.9 M and 8.6 kJ mol^{-1} respectively for FHD). This implies that LZ-END is more stable than FHD. The *m*-value informs us of the cooperativity of the unfolding transition. For the FHD, the *m*-value is 4.3 kJ mol^{-1} M^{-1} and for LZ-END it is 3.0 kJ mol^{-1} M^{-1}. This suggests that the FHD construct is more compact in the native conformation than the LZ-END, or alternatively, that LZ-END is less homogenous than the FHD.

The circular dichroism monitored unfolding curves are different for the two constructs. While the FHD continues to demonstrate two-state unfolding, the LZ-END clearly follows a three-state unfolding pathway and a near native intermediate species (I) is detectable. The thermodynamic parameters obtained from the fits to the unfolding curves show a decreased ΔGH_2O for the FHD construct when probed with circular dichroism compared to the fluorescence-monitored transition with a value of 2.4 kJ mol^{-1}. The *m*-value remains similar for both the fluorescence and circular dichroism-monitored transitions. The three-state transition for the LZ-END construct shows a higher $\Delta G(H_2O)$ for the I→D transition (11.6 kJ mol^{-1} compared to 7.7 kJ mol^{-1} for the N→I transition). Similarly, the *m*-value is higher for the I→D transition with a value of 4.4 kJ mol^{-1} M^{-1} compared to 3.7 kJ mol^{-1} M^{-1} for the N→I transition. This implies that the greatest exposure of surface area to solvent happens upon the I→D transition which is consistent with the unfolding of the protein along this transition.

4 | DISCUSSION

The research undertaken in this study assesses the role of the FOXP2 leucine zipper as it cooperates with the FHD to bind DNA and hence execute transcriptional function. Partitioning the structural and functional contributions of the leucine zipper domain, FHD, and the flanking unstructured regions in the absence and presence of DNA provides both a global and local perspective on the cooperativity between these domains in terms of their interaction with each other and their capacity for DNA-binding. It is important to know the precise roles of the various regions of the FOXP2 sequence as it

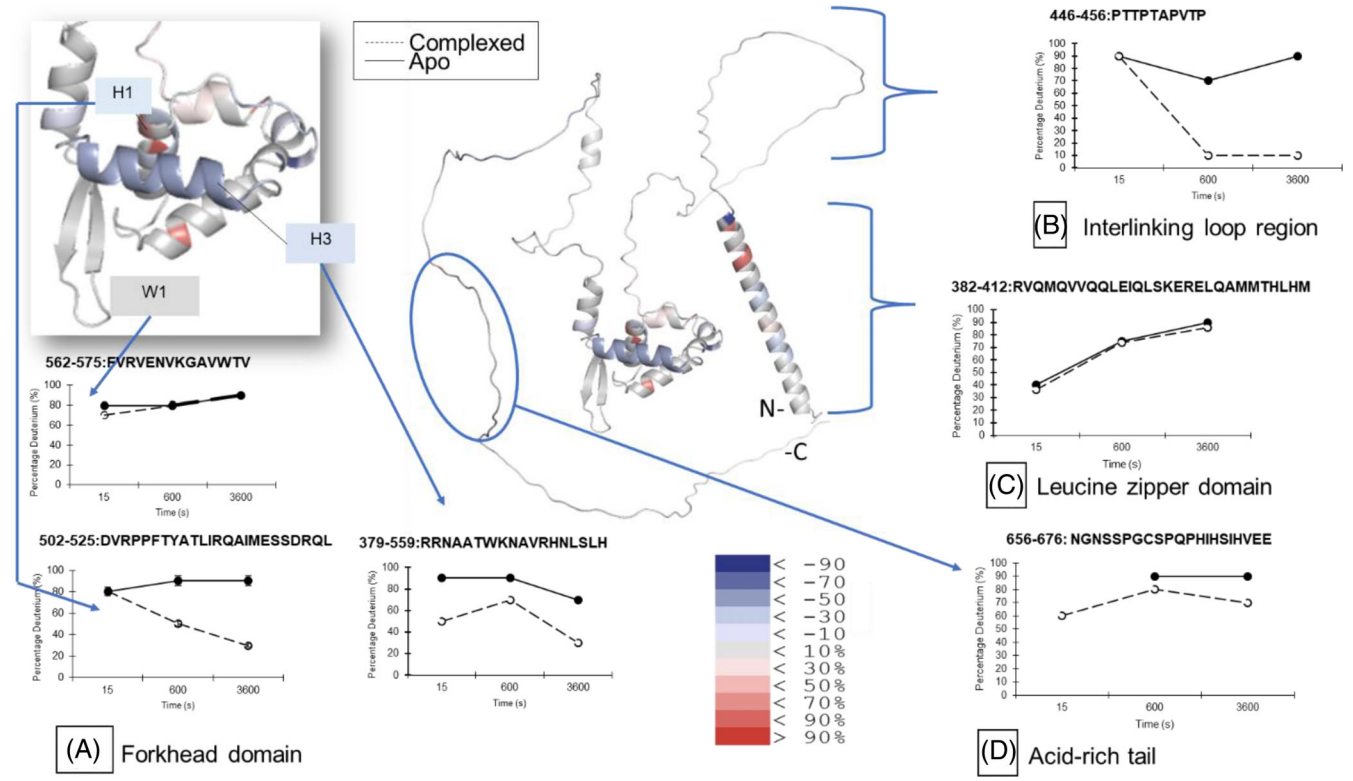

FIGURE 7 Hydrogen/deuterium exchange difference maps comparing the level of deuteration of LZ-END in the absence and presence of DNA. Heat maps generated from hydrogen exchange mass spectrometry of the apo and complexed (DNA-bound) LZ-END constructs are mapped to the AlphaFold FOXP2 structure to visually represent the time-based dynamics of key regions within this construct. The map is colored from red to blue where red represents highly deuterated regions and blue represents regions of the backbone that are more protected from exchange. Deuterium uptake plots for relevant regions are shown and compare the DNA–protein complex (dashed line) with the apo protein (continuous line) over 15, 600, and 3600 s time intervals. (A) Helix-3 (the DNA recognition helix) and H1 in the forkhead domain display decreased levels of exchange upon binding to DNA as compared to the more dynamic apo form, while the dynamics of wing-1 are unchanged by DNA. (B) The interlinking loop region is highly dynamic in the apo form but sees an increase in protection from exchange upon DNA-binding, especially at the region *PTTPTAPVTP*. (C) DNA-binding does not induce significant changes in the structural dynamics of the leucine zipper domain overall, although the general trend is an increase in deuteration over time. (D) The acid-rich tail shows increased protection from exchange in the presence of DNA.

enhances our comprehension of FOXP2's molecular function. This information is valuable for deciphering the broader regulatory networks and functional consequences of FOXP2 activity.

The two constructs used in this study were the isolated FHD and the LZ-END constructs and they were chosen because both the FHD and the LZ have been implicated in both DNA binding and oligomerization. In this work, we investigated the dynamics, DNA binding and stability of these two constructs in order to understand more about the individual contributions of the two most structured domains in this protein both to DNA binding and to stability, dynamics and fold of the protein.

Structurally, the circular dichroism results confirm that both constructs are predominantly helical, and the fluorescence results show that the FHD in both regions is folded similarly with buried tryptophan residues (Figure 3). When the protein is bound to DNA, the fold of the FHD does not change, but there do seem to be some subtle changes in the backbone of possibly the more disordered regions as seen by slight differences to the circular dichroism spectra although both constructs do remain helical (Figure 3).

Despite the fact that the FHD is capable of forming domain swapped dimers,[24] under the conditions and concentrations used in our study, the isolated FHD remains entirely monomeric and exists as a single species. The LZ-END construct, on the other hand, exists as a mixture of two species that likely represent a dimer and a trimer (Figure 4).

Looking at the quaternary structure in relation to DNA binding in the EMSA (Figure 5), we can see that while the FHD binds DNA as a single species, arguably the same monomeric species detected with size exclusion chromatography, the LZ-END construct clearly binds as three different species. This means that the two species that are detected in solution both bind independently to DNA and in addition to this, there is a third species bound to DNA that is not seen in the apo state. The appearance of a third DNA-bound species on the EMSA could mean one of two things. Either (i) DNA induces a conformational change or oligomerization event to form a third species (in addition to the dimer-like and trimer-like oligomeric species) and all three species can bind DNA, or (ii) DNA can bind one of the two species with a stoichiometry greater than 1. This second scenario could

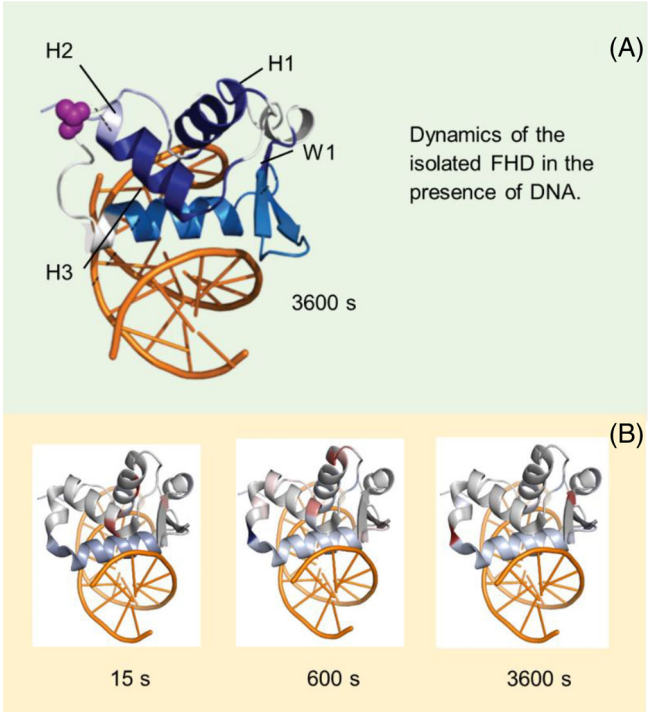

FIGURE 8 Comparing the conformational dynamics of the isolated FHD and the forkhead domain present in the LZ-END construct when in the presence of DNA. (A) The conformational dynamics of the isolated FHD bound to DNA was mapped to the crystal structure (PDB: 2A07) and is shown here at the full duration of exchange, with most secondary structure features shown to be highly protected from exchange in the presence of DNA.[23] (B) Comparatively, the FHD in the longer LZ-END variant, demonstrates a significant amount of protection for helix-3 and helix-1 while the remainder of the FHD seems to show almost no change in dynamics in the presence of DNA.

be a possibility if the FHD forms a domain swapped dimer as this presents two DNA binding helices per dimer. In either scenario, it appears that the presence of DNA induces a change in the oligomeric state of the LZ-END construct, and this might be important for FOXP2's mechanism of regulation of transcription. Despite this change in oligomeric state in the presence of DNA, we do not see a significant change in secondary or tertiary structure, meaning that the overall fold has not changed, and the protein is simply oligomerizing at the LZ or FHD. Since the isolated FHD does not form oligomers (Figure 4), it is plausible that the oligomerization detected in the LZ-END species EMSA is happening at the LZ domain rather than the FHD. Our results correspond with a similar study performed on FOXP3[31] where it was shown that FOXP3 FHD remains monomeric and FOXP3 dimerizes via the leucine zipper and interlinking region. Our work also corresponds with work done on FOXP1[32] which suggested that dimer formation was improved by the presence of the LZ region.

Study of DNA binding using fluorescence anisotropy (Figure 6) also shows a difference between LZ-END and FHD. LZ-END binds to the DNA with greater affinity than the FHD alone. This means that despite the fact that the FHD is the DNA binding domain, the LZ (and/or the interlinking random coiled region) is also involved in DNA binding and contributes to the affinity of binding.

In order to understand deeper, the interaction of this protein with DNA, we compared the dynamics of the LZ-END construct in the presence and absence of DNA. Most of the protein does not show a difference in backbone exchange whether in the apo or DNA bound forms, however there are certain regions that have been highlighted in the difference map in Figure 7 that do show a difference.

The FHD shows the most pronounced difference, particularly in H1 and H3 which both become more protected from exchange upon DNA binding. This means that these regions are directly involved in DNA binding which is to be expected as H3 is known to be the DNA binding helix for the winged helix fold of all FHDs.[6] This result is similar to what we have shown previously with a hydrogen exchange study of the isolated FHD.[25]

The hydrogen exchange results for FHD and LZ-END are not identical however, and differences are seen when comparing the backbone dynamics of the isolated FHD to that of the FHD in the LZ-END construct. In the isolated FHD, there is not only increased protection at H3 and H1 but also at W1 and H2 upon DNA binding (Figure 8). This is not seen in the LZ-END complex, and this implies that the DNA–FHD interface in the larger LZ-END complex is smaller than in the isolated FHD, likely due to the additional sequence and the fold of the structure. Despite these restrictions on where the DNA and protein can interact, the affinity for the DNA is larger in the LZ-END construct which suggests that regions of the protein other than the FHD are involved in DNA binding affinity.

Interestingly, two regions of random coil sequence show an increase in backbone protection upon DNA binding. They are the interlinking loop region and a portion of the C-terminal tail just preceding the acid-rich region. The hydrogen exchange results suggest that these two regions change in dynamics upon DNA binding. This result implies that they may be directly involved in DNA binding or, as had been suggested previously for the acid rich tail,[19] they may be sites of oligomerization. This is consistent with the EMSA results and the idea that DNA binding induces an oligomeric event at these regions. These two regions are likely to be responsible for the increased affinity for DNA of this construct compared to the isolated FHD.

The leucine zipper itself does not show a difference in deuteration in the presence and absence of DNA which suggests that DNA does not bind to the LZ region directly and nor is there a change in oligomeric state at the LZ upon DNA binding. It is likely that the LZ remains an oligomeric interface in the presence and absence of DNA. What we do see, however, is a clear increase in deuteration of the LZ region over time. This implies that the LZ region is highly dynamic and despite its structure, it is accessible to the solvent.

Finally, we also compared the equilibrium unfolding curves of both FHD and the LZ-END, to understand what effect the LZ has on the stability of the DNA binding domain. Since the only tryptophan residues in this protein are in the FHD, it is not surprising that when using fluorescence to probe unfolding, both the two constructs appear to unfold in a similar manner. This means that the FHD retains

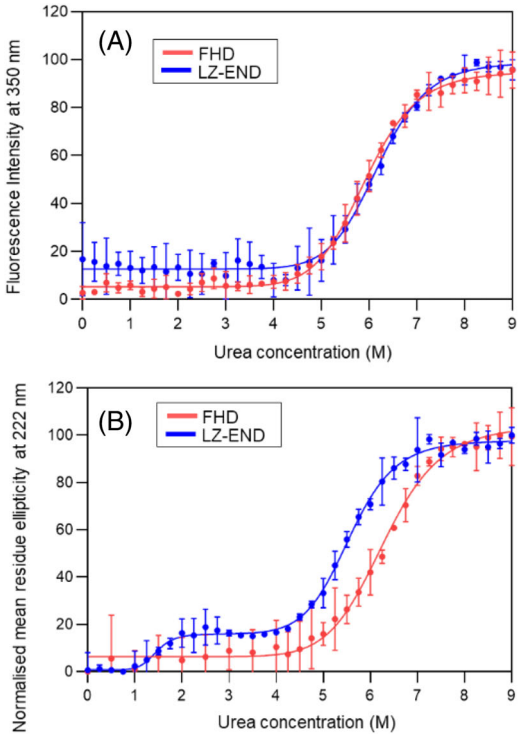

(C)

	Unfolding using fluorescence as probe			Unfolding using circular dichroism as probe		
	ΔG_{H2O} (kJ.mol^{-1})	Cm (M)	*m*-value (kJ.mol^{-1}.M^{-1})	ΔG_{H2O} (kJ.mol^{-1})	Cm (M)	*m*-value (kJ.mol^{-1}.M^{-1})
FHD	8.63 ± 0,67	5.9 ± 0.45	4.3 ± 0.32	2.37 ± 0.94	6.2 ± 0.56	3.8 ± 0.64
LZ-END (N→I)				7.7 ± 0.32	1.5 ± 0.47	3.7 ± 0.85
LZ-END (I→D)	19.89 ± 0.54	6.2 ± 0.63	3.0 ± 0.43	11.59 ± 0,84	5.6 ± 0.65	4.4 ± 0.76

FIGURE 9 The equilibrium unfolding curves of the LZ-END and FHD at the tertiary and secondary structural level. Urea-induced equilibrium unfolding was monitored via intrinsic tryptophan fluorescence at 350 nm (A) and by circular dichroism ellipticity at 222 nm (B). The constructs were denatured using increasing concentrations of urea (0–9 M). While the equilibrium unfolding curves for both the FHD (red) and LZ-END (blue) fit to a two-state model when fluorescence is used as a probe, unfolding monitored using circular dichroism fits a 2-state model for FHD (red) but a 3-state model for the LZ-END (blue). The thermodynamic parameters obtained by the fits to the data are shown in (C).

its stability and fold in the longer protein which confirms the results of the structural studies. The curves were fit to a two-state model, and we see that both the *Cm* and *m*-value are similar for both constructs, implying that the FHD is similar in both stability and fold (compactness) in both constructs. The ΔGH_2O calculated for LZ-END is more than double that of the FHD which likely refers to additional stabilizing interactions that form in the larger construct.

When equilibrium unfolding was performed by probing changes in ellipticity (which indicates the level of secondary structure) with increases in denaturant concentration, we see that there are distinct differences in the two constructs. While the FHD continues to unfold in a simple two-state manner (N→D), the LZ-END now shows a three-state unfolding transition with a near native stable intermediate species being detected at equilibrium. This intermediate may represent the dissociation of the oligomeric species to their monomeric form prior to unfolding.

The equilibrium unfolding results point to the uncoupling of the FHD from the LZ upon unfolding and further support our conclusions that it is the LZ and possibly the other random coil regions of the protein that are responsible for oligomerization and not the FHD.

In summary, we show here that the LZ and FHD function in a cooperative way to regulate DNA binding specificity and affinity. They do not do this in isolation, however and disordered regions in the FOXP2 sequence, particularly the interlinking loop between the LZ and FHD and parts of the C-terminal tail, play a significant role in DNA binding and oligomerization of FOXP2.

Our work agrees with a similar study performed on FOXP1[32] which concluded that the interdomain linker between the LZ and FHD of FOXP1 was a critical player in the protein's stability, dimerization and DNA binding activity. These results emphasize the significance of the unstructured regions of FOXP proteins in their structure and function.

5 | CONCLUSION

In this study we sought to compare the DNA-binding capabilities, conformational dynamics and stability of the FOXP2 FHD and leucine zipper domain. Considering these two domains are both associated with DNA binding and oligomerization, their individual and cooperative impact on FOXP2 structure and function was assessed in the absence and presence of DNA. This study showed for the first time that DNA can bind to multiple species of FOXP2, and that DNA binding induces a conformational change in the oligomeric structure of FOXP2 to form a DNA-bound oligomer that does not exist in the apo state. Taken in combination with the dynamics studies, the region involved in this oligomerization event appears to be the interlinking loop region and the C-terminal tail. This result suggests that oligomerization may be employed in the transcriptional regulatory mechanism of this protein. Indeed, the higher order structures that form in the LZ-END construct are also capable of binding DNA with greater affinity than the isolated FHD, highlighting their significance. The stability studies show that in

the folded, stable structure, the LZ and FHD cooperate with each other and need to be uncoupled in order for the protein to unfold. Taken together these results highlight the importance of oligomerization and interplay between the domains in order to regulate DNA binding. In essence, unraveling the precise roles of the different domains in FOXP2 enhances our comprehension of its molecular function, opening avenues for therapeutic interventions, insights into speech and language disorders, and a deeper understanding of its intricate molecular mechanisms which lays the groundwork for future studies in transcriptional regulation and functional dynamics.

AUTHOR CONTRIBUTIONS

Sylvia Fanucchi: Conceptualization; investigation; funding acquisition; writing – review and editing; formal analysis; project administration; supervision; resources. **Cardon Maria Perumal:** Investigation; writing – original draft; formal analysis; data curation. **Monare Thulo:** Investigation; data curation. **Sindisiwe Buthelezi:** Investigation; writing – review and editing; data curation. **Previn Naicker:** Methodology. **Stoyan Stoychev:** Methodology. **Aasiya Lahki:** Investigation; data curation.

ACKNOWLEDGEMENTS

We are grateful to Jessica Brothwell from the University of the Witwatersrand for providing data towards one of the figures.

PEER REVIEW

The peer review history for this article is available at https://www.webofscience.com/api/gateway/wos/peer-review/10.1002/prot.26699.

DATA AVAILABILITY STATEMENT

The data that support the findings of this study are available from the corresponding author upon reasonable request.

ORCID

Sylvia Fanucchi https://orcid.org/0000-0002-2537-1065

REFERENCES

1. Weigel D, Jürgens G, Küttner F, Seifert E, Jäckle H. The homeotic gene fork head encodes a nuclear protein and is expressed in the terminal regions of the drosophila embryo. *Cell*. 1989;57(4):645-658.
2. Latchman DS. Eukaryotic transcription factors. *Biochem J*. 1990;270 (2):281-289.
3. Latchman DS. Transcription factors: an overview. *Int J Exp Pathol*. 1993;74(5):417-422.
4. Suter DM. Transcription factors and DNA play hide and seek. *Trends Cell Biol*. 2020;30(6):491-500.
5. Benayoun BA, Caburet S, Veitia RA. Forkhead transcription factors: key players in health and disease. *Trends Genet*. 2011;27(6):224-232.
6. Hackett BP. *Fox transcription factors*. Wiley Encyclopedia of Molecular Medicine; 2002.
7. Hannenhalli S, Kaestner KH. The evolution of FOX genes and their role in development and disease. *Nat Rev Genet*. 2009;10(4):233-240.
8. Katoh M, Katoh M. Human FOX gene family. *Int J Oncol*. 2004;25(5): 1495-1500.
9. Jackson BC, Carpenter C, Nebert DW, Vasiliou V. Update of human and mouse forkhead box (FOX) gene families. *Hum Genomics*. 2010;4 (5):345-352.
10. Sin C, Li H, Crawford DA. Transcriptional regulation by FOXP1, FOXP2, and FOXP4 dimerization. *J Mol Neurosci*. 2015;55(2):437-448.
11. Belton E, Salmond CH, Watkins KE, Vargha-Khadem F, Gadian DG. Bilateral brain abnormalities associated with dominantly inherited verbal and orofacial dyspraxia. *Hum Brain Mapp*. 2003;18(3):194-200.
12. Lai CS, Gerrelli D, Monaco AP, Fisher SE, Copp AJ. FOXP2 expression during brain development coincides with adult sites of pathology in a severe speech and language disorder. *Brain*. 2003;126(11):2455-2462.
13. Vernes SC, Fisher SE. Genetic pathways implicated in speech and language. *Animal models of speech and language disorders*. Springer science; 2013:13-40.
14. Feuk L, Kalervo A, Lipsanen-Nyman M, et al. Absence of a paternally inherited FOXP2 gene in developmental verbal dyspraxia. *Am J Hum Genet*. 2006;79(5):965-972.
15. Estruch SB, Graham SA, Quevedo M, et al. Proteomic analysis of FOXP proteins reveals interactions between cortical transcription factors associated with neurodevelopmental disorders. *Hum Mol Genet*. 2018;27(7):1212-1227.
16. Li X, Han M, Zhang H, et al. Structures and biological functions of zinc finger proteins and their roles in hepatocellular carcinoma. *Biomarker Res*. 2022;10:1-13.
17. Takahashi H, Takahashi K, Liu FC. FOXP genes, neural development, speech and language disorders. *Forkhead transcription factors: vital elements in biology and medicine*. Springer; 2010:117-129.
18. Li S, Weidenfeld J, Morrisey EE. Transcriptional and DNA binding activity of the Foxp1/2/4 family is modulated by heterotypic and homotypic protein interactions. *Mol Cell Biol*. 2004;24(2):809-822.
19. Thulo M, Rabie MA, Pahad N, et al. The influence of various regions of the FOXP2 sequence on its structure and DNA-binding function. *Biosci Rep*. 2021;41(1):BSR20202128.
20. Erlanson DA, Chytil M, Verdine GL. The leucine zipper domain controls the orientation of AP-1 in the NFAT· AP-1· DNA complex. *Chem Biol*. 1996;3(12):981-991.
21. Luscombe NM, Austin SE, Berman HM, Thornton JM. An overview of the structures of protein–DNA complexes. *Genome Biol*. 2000;1:1-37.
22. Webb H, Steeb O, Blane A, et al. The FOXP2 forkhead domain binds to a variety of DNA sequences with different rates and affinities. *J Biochem*. 2017;162(1):45-54.
23. Donald HL, Blane AA, Buthelezi S, et al. Assessing the dynamics and macromolecular interactions of the intrinsically disordered protein YY1. *Biosci Rep*. 2023;43(10):BSR20231295.
24. Stroud JC, Wu Y, Bates DL, et al. Structure of the forkhead domain of FOXP2 bound to DNA. *Structure*. 2006;14(1):159-166.
25. Morris G, Stoychev S, Naicker P, Dirr HW, Fanucchi S. The forkhead domain hinge-loop plays a pivotal role in DNA binding and transcriptional activity of FOXP2. *Biol Chem*. 2018;399(8):881-893.
26. Nelson CS, Fuller CK, Fordyce PM, Greninger AL, Li H, DeRisi JL. Microfluidic affinity and ChIP-seq analyses converge on a conserved FOXP2-binding motif in chimp and human, which enables the detection of evolutionarily novel targets. *Nucleic Acids Res*. 2013;41(12): 5991-6004.
27. Pace CN, Scholtz JM. Measuring the conformational stability of a protein. *Protein structure: a practical approach*. FEBS press. Vol 2; 1997: 299-321.
28. Jumper J, Evans R, Pritzel A, et al. Highly accurate protein structure prediction with AlphaFold. *Nature*. 2021;596(7873):583-589.
29. Perumal K, Dirr HW, Fanucchi S. A single amino acid in the hinge loop region of the FOXP forkhead domain is significant for dimerisation. *Protein J*. 2015;34(2):111-121.
30. Morris G, Fanucchi S. A key evolutionary mutation enhances DNA binding of the FOXP2 forkhead domain. *Biochemistry*. 2016;55(13): 1959-1967.
31. Leng F, Zhang W, Ramirez RN, et al. The transcription factor FoxP3 can fold into two dimerization states with divergent implications for regulatory T cell function and immune homeostasis. *Immunity*. 2022; 55(8):1354-1369.

32. Cruz P, Paredes N, Asela I, et al. Domain tethering impacts dimerization and DNA-mediated allostery in the human transcription factor FoxP1. *J Chem Phys*. 2023;158:195101.

SUPPORTING INFORMATION

Additional supporting information can be found online in the Supporting Information section at the end of this article.

How to cite this article: Perumal CM, Thulo M, Buthelezi S, et al. Unraveling the interplay between the leucine zipper and forkhead domains of FOXP2: Implications for DNA binding, stability and dynamics. *Proteins*. 2024;1-13. doi:10.1002/prot.26699